The Astrophysical Journal Letters, 751:L40 (5pp), 2012 June 1 doi:10.1088/2041-8205/751/2/L40

SOFT X-RAY IRRADIATION OF H_2S ICE AND THE PRESENCE OF S_2 IN COMETS

A. Jiménez-Escobar[1], G. M. Muñoz Caro[1], A. Ciaravella[2], C. Cecchi-Pestellini[3], R. Candia[2], and G. Micela[2]
[1] Centro de Astrobiología (CSIC-INTA), Carretera de Ajalvir, km 4, Torrejón de Ardoz, 28850 Madrid, Spain; munozcg@cab.inta-csic.es
[2] INAF-Osservatorio Astronomico di Palermo, P.za Parlamento 1, 90134 Palermo, Italy
[3] INAF-Osservatorio Astronomico di Cagliari, Strada n.54, Loc. Poggio dei Pini, I-09012 Capoterra (CA), Italy
Received 2012 March 14; accepted 2012 May 1; published 2012 May 16

ABSTRACT

Little is known about the effects of X-rays in interstellar ices. To understand the sulfur depletion in dense clouds and the presence of S_2 in comets, we simulated experimentally the soft X-ray processing (0.3 keV) of H_2S ice for the first time. Experiments were performed under ultrahigh vacuum conditions at 8 K using infrared and quadrupole mass spectrometry to monitor the solid and gas phases, respectively. A UV irradiation experiment using a similar dose was made for comparison. After X-ray irradiation, an infrared absorption appears near 4.0 μm which is attributed to H_2S_2 formation in the ice. This identification is also supported by the desorption at 133 K of m/z 66, 65, 64, corresponding to the mass fragments of H_2S_2. The H_2S_2 species is expected to be present in interstellar and cometary ices that were processed by X-rays. Further irradiation leads to dissociation of this molecule forming S_2 and larger S-molecules up to S_8, which may explain the depletion of sulfur in dense clouds. CS_2 was so far the parent molecule proposed for S_2 formation in comets. But the abundance of H_2S_2, formed by irradiation of pure H_2S or H_2S in an H_2O–ice matrix, should be larger than that of CS_2 in the ice, the latter requiring a carbon source for its formation. Based on our experimental results, we propose that S_2 in comets could be formed by dissociation of H_2S_2 in the ice.

Key words: ISM: molecules – methods: laboratory – X-rays: ISM

1. INTRODUCTION

Sulfur is depleted in dense clouds, Class 0 and Class I sources (e.g., Buckle & Fuller 2003), and hot cores (Wakelam et al. 2004). Because of the high hydrogen abundances and the mobility of hydrogen in the ice matrix, sulfur atoms impinging in interstellar and circumstellar ice mantles are expected to form H_2S preferentially. There are only upper limits of the solid H_2S abundance (e.g., Jiménez-Escobar & Muñoz Caro 2011), and the only S-bearing molecule unambiguously detected in ice mantles is OCS, because of its large band strength in the infrared (Geballe et al. 1985; Palumbo et al. 1995) and maybe SO_2 (Boogert et al. 1997). OCS is formed by UV or ion irradiation of H_2S ice containing CH_3OH or CO (Ferrante et al. 2008; Garozzo et al. 2010). Upon UV irradiation, H_2S is also the precursor of more complex species such as S-polymers (Jiménez-Escobar & Muñoz Caro 2011), which could be the reservoir of the depleted sulfur (Wakelam et al. 2005; Garozzo et al. 2010).

The most abundant interstellar ice molecules are common to cometary ices (e.g., Bockelée-Morvan et al. 2000). Therefore, the abundance of H_2S in comets, up to 1.5% relative to H_2O as inferred from millimeter and submillimeter observations (Bockelée-Morvan et al. 2000, 2010; Boissier et al. 2007), also suggests that this molecule should be present in interstellar icy grain mantles. Other S-species (CS_2, SO_2, OCS, and H_2CS) were detected in comet Hale–Bopp with abundances between 0.02% and 0.4% (Bockelée-Morvan et al. 2000). Observations of S_2 in the coma of comet IRAS-Araki-Alcock showed that this species came from, or very close to, the nucleus (A'Hearn et al. 1983). Later, S_2 was tentatively detected in comet Hyakutake and is probably ubiquitous in comets, but its detection requires a sufficiently short distance from the comet to Earth (Laffont et al. 1996). The origin of S_2 in comets is unclear (Bockelée-Morvan et al. 2004). The reactions induced by ions or UV photons in ices containing H_2S were studied experimentally (e.g., Grim & Greenberg 1987; Moore et al. 2007; Ferrante et al. 2008; Garozzo et al. 2010; Jiménez-Escobar & Muñoz Caro 2011). But no experiments were dedicated to study X-ray irradiation of H_2S ice. X-rays could play a significant role in energetic ice processing in various astrophysical environments such as circumstellar regions around protostars and young solar-type stars, especially when the X-ray flux exceeds the UV flux (Ribas et al. 2005). We report here the irradiation of pure H_2S ice with soft X-rays of 0.3 keV to explore the role played by X-rays in the formation of other S-bearing molecules in icy environments. In particular, we discuss the possible contribution of X-rays to the formation of S_2 in comets. The low flux of our X-ray source mimics more realistic astrophysical conditions and its spectrum peaked at 0.3 keV matches the peak of the quiet X-ray emission of today's Sun. Such a low flux demands long irradiation times of one day, sensitive detection techniques, and optimum ultrahigh vacuum conditions to detect irradiation products unambiguously.

Section 2 describes the experimental protocol and Section 3 reports the results. The conclusions and astrophysical implications are presented in Section 4.

2. IRRADIATION EXPERIMENTS

The experiments were performed using the Interstellar Astrochemistry Chamber (ISAC). This setup and the standard experimental protocol are described in Muñoz Caro et al. (2010). ISAC is an ultrahigh vacuum chamber, with pressure in the range $P = (2.5–4.0) \times 10^{-11}$ mbar, where an ice layer is made by deposition of a gas mixture onto a cold finger at 8 K. The ice is monitored in situ by a transmittance Fourier Transform Infrared (FTIR) spectrometer, and the volatile species are detected by a Quadrupole Mass Spectrometer (QMS). Solid H_2S (Praxair 99.8%) was irradiated using an electron impact X-ray source built at the X-ray Astronomy Calibration and Testing facility of the INAF–Osservatorio Astronomico di Palermo. The X-ray flux at the sample position was 6.1×10^9 photons cm^{-2} s^{-1}

Table 1
Log of Experiments

Exp. No.	$N(H_2S)$ (cm^{-2})	E Fluence (photons cm^{-2})	Restricted Dose (eV $molec^{-1}$)	$N(H_2S_2)$ (cm^{-2})	$\frac{N(H_2S_2)}{N(H_2S)}$
1. Blank	2.6×10^{18}	...	...	0.0	0.0
2. X-ray	2.9×10^{18}	1.2×10^{17}	0.033[a]	8.3×10^{15}	2.9×10^{-3}
3. X-ray	2.6×10^{18}	1.5×10^{17}	0.046[a]	8.6×10^{15}	3.3×10^{-3}
4. UV	6.9×10^{17}[a]	6.9×10^{16}	0.10	1.7×10^{16}	2.5×10^{-2}

Note.
[a] This value of the column density corresponds to an absorption of about 99% of the incident UV photons. The column density of the deposited H_2S ice was about a factor of three larger.

corresponding to 2.3×10^{12} eV cm^{-2} s^{-1}. The X-ray spectrum was obtained with a C anode and has a main peak at the C Kα line and a tail at higher energies due to the bremsstrahlung continuum above the absorption edge (see Figure 1 of Ciaravella et al. 2011). Although the absorption edge of the sulfur K shell is at ~2.5 keV, where the X-ray flux of our lamp is negligible, the L shell of sulfur atoms can efficiently be ionized given their large photoelectric cross-section around the C Kα line threshold.

H_2S was deposited with a rate of 1.8 ML s^{-1} where one monolayer (ML) corresponds to a column density of 1.0×10^{15} molecules cm^{-2}. After irradiation, the ice is warmed up at a constant rate of 1 K min^{-1}. FTIR spectra with a spectral resolution of 1 cm^{-1} were acquired before and after irradiation, as well as during warm-up every 10 K. The ice molecules desorbing inside the chamber during warm-up were continuously monitored by QMS.

3. RESULTS

The log of experiments is given in Table 1. Experiment N1 is a blank using the same experimental protocol as the X-ray experiments, but with no irradiation, while N2 and N3 involved X-ray irradiation of the H_2S ice. For comparison we also performed a UV irradiation experiment, N4, using a microwave-stimulated hydrogen flow discharge lamp with a UV photon flux of 2.5×10^{14} photons cm^{-2} s^{-1} at the sample position (Muñoz Caro et al. 2010). While the irradiation time in X-ray experiments was close to 24 hr, in the UV experiment the total irradiation time was only 30 s to obtain a dose comparable to that of the X-ray experiments.

The column density of the deposited ice, $N(H_2S)$ in the second column of Table 1, was calculated using the formula

$$N = \int_{\Delta\nu} \frac{\tau_\nu d\nu}{A}, \quad (1)$$

where N is the column density in cm^{-2}, τ_ν is the optical depth of the band, $d\nu$ is the wavenumber differential in cm^{-1}, and A is the band strength in cm $molecule^{-1}$. The adopted band strength for H_2S at 8 K is $A(H_2S) = 2.0 \times 10^{-17}$ cm $molecule^{-1}$ (Jiménez-Escobar & Muñoz Caro 2011). The photon fluence, in photons cm^{-2}, is given by the product $I_0 \cdot t$, where I_0 is the photon flux and t is the irradiation time. For the X-ray and UV experiments, the energy fluence expressed in eV cm^{-2}, third column of Table 1, is obtained by integrating the emission spectra of the X-ray and UV lamps, respectively. By taking into account the absorbance of the ice at different energies, the total energy absorbed by the ice during the X-ray irradiation was $\mathcal{E}_{abs} = 9.8 \times 10^{16}$ and 1.2×10^{17} eV cm^{-2} in the N2 and N3 experiments, respectively. The restricted dose $\mathcal{D}$ in absorbed eV $molecule^{-1}$, fourth column of Table 1, was obtained from

$$\mathcal{D} = \frac{\mathcal{E}_{abs}}{N(H_2S)} \quad (2)$$

in these experiments. The UV absorption cross-section of solid H_2S is unknown. As an approximation, we adopted the Lyα cross-section for H_2S in the gas phase, 9.01×10^{-16} cm^2 nm (Lee et al. 1987) in the spectral range of the UV lamp [121.2–159.3 nm] corresponding to 6.7×10^{-18} cm^2 per photon of average energy 9.2 eV. That value corresponds to an absorption of 99% of the impinging photons for $N(H_2S) = 6.9 \times 10^{17}$ molecules cm^{-2}. The restricted dose for the UV experiment given in the fourth column of Table 1 was estimated using the above $N(H_2S)$ value. The fifth column in Table 1 provides the column density of H_2S_2, $N(H_2S_2)$, formed by X-ray or UV irradiation of H_2S ice. This value divided by the column density of H_2S, $N(H_2S)$ from the second column, is given in the last column of Table 1.

Figure 1 displays the infrared spectra of pure H_2S upon X-ray irradiation (top panels), UV irradiation (middle panels), and the blank experiment with no irradiation (bottom panels); see the caption for explanation. During irradiation, a new band at 2501 ± 4 cm^{-1} (4.0 μm) appears in both the X-ray and the UV experiments, attributed by Isoniemi et al. (1999) to complexes of H_2S_2, probably the H_2S_2–H_2S complex. The reaction scheme induced by X-rays is probably similar to that induced by UV photons. The process begins with $HS^{\cdot}$ radical formation as

$$H_2S + h\nu \rightarrow HS^{\cdot} + H^+ + e^-, \quad (3)$$

followed by the reaction of two $HS^{\cdot}$ radicals

$$HS^{\cdot} + HS^{\cdot} \rightarrow H_2S_2. \quad (4)$$

The H_2S_2 molecule is expected to be formed by X-ray irradiation in our experiments rather than $HS_2^{\cdot}$ at 2483 cm^{-1} (Jiménez-Escobar & Muñoz Caro 2011) due to the very low dose employed, as it occurs with the UV experiment we report here using a comparable low dose. If the dose is increased, H_2S_2 is subsequently photolyzed yielding $HS_2^{\cdot}$; see the top panel of Figure 6 of Jiménez-Escobar & Muñoz Caro (2011), following the reaction scheme of Isoniemi et al. (1999). The integrated absorbances of H_2S_2 for X-ray experiments N2 and N3 of Table 1 are 0.072 and 0.075 cm^{-1}, corresponding to dose values of 0.033 and 0.046 eV $molecule^{-1}$. The integrated absorbance of H_2S_2 produced in the UV experiment was 0.144 cm^{-1} corresponding to experiment N4 of Table 1 for a dose of 0.10 eV $molecule^{-1}$. Therefore, since a linear dependence of the integrated absorbance with the dose was observed for restricted dose values below 0.1 eV $molecule^{-1}$, it is possible to

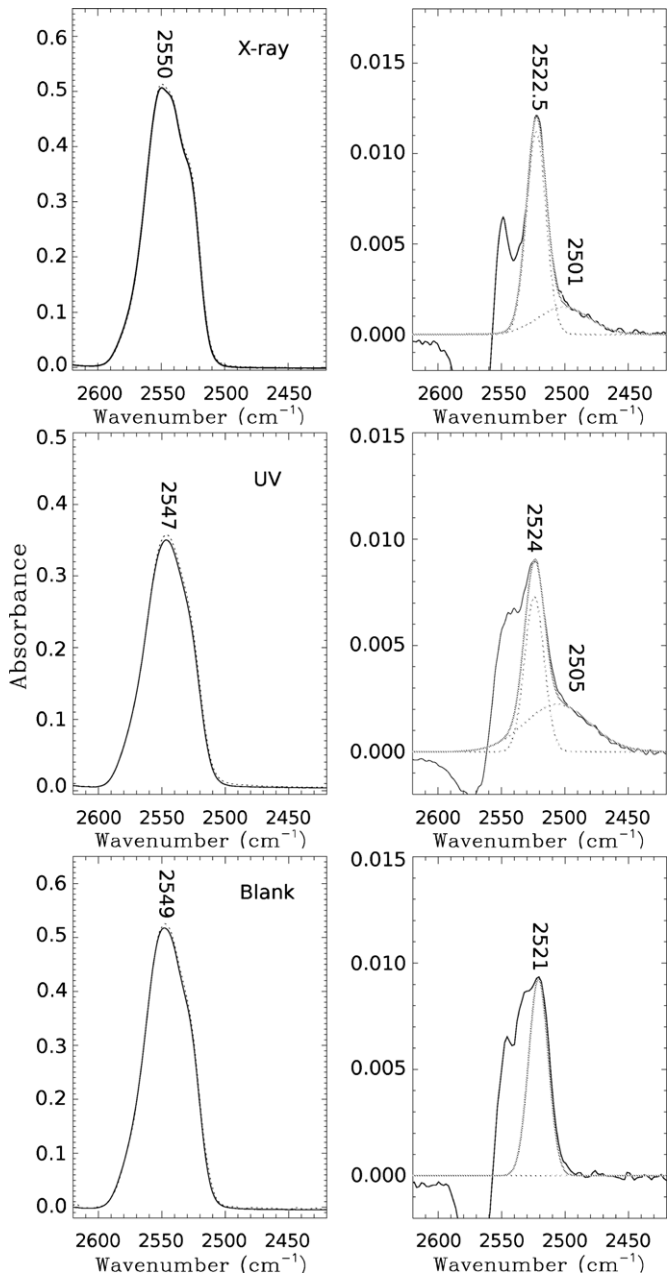

Figure 1. Infrared spectra of experiments N3 (X-ray irradiation), N4 (UV irradiation), and N1 (blank with no irradiation); see Table 1. Left panels show the absorption band of deposited H_2S ice (solid line), and after irradiation for the X-ray and UV experiments (dotted line), showing little difference due to the low dose of irradiation. Right panels show the subtraction of the spectra made after and before irradiation displayed in the left panels (solid line). Deconvolutions using two Gaussians are superposed (dotted lines) and the best fit made by addition of the two Gaussians (gray line).

extrapolate those results to the same dose value in experiments N2 and N3 for X-rays, and N4 for UV, we obtain a ratio of

$$\frac{A_{\rm int}(H_2S_2, {\rm X-ray})}{A_{\rm int}(H_2S_2, {\rm UV})} = \begin{cases} 1.5 \text{ for N2} \\ 1.1 \text{ for N3} \end{cases}, \quad (5)$$

where $A_{\rm int}(H_2S_2)$ is the integrated absorbance. This indicates that the production yield of H_2S_2 is similar in the UV and X-ray experiments, but there can be an important error in this value introduced by the estimated value of the dose in the UV experiment, which depends on the value of $N(H_2S)$ corresponding to 99% UV absorption. This value cannot be

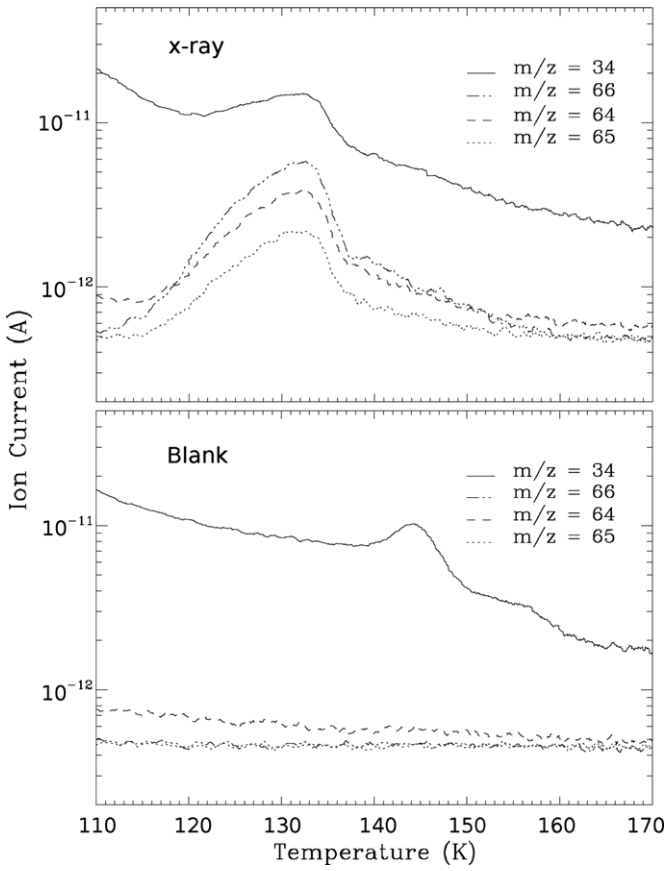

Figure 2. TPD curves corresponding to X-ray irradiation of H_2S ice, experiment N3 of Table 1 (top panel) and the blank with no irradiation, experiment N1 (bottom panel). The traces, in order of decreasing ion current, correspond to the tail of the desorption of H_2S ($m/z = 34$) and the m/z values 66, 64, and 65 for the desorption of the H_2S_2 product near 133 K in the X-ray experiment. The peaks superposed on the desorption tail of H_2S ($m/z = 34$) are due to H_2S co-desorption induced by the release of H_2S_2 in the X-ray experiment, and co-desorption with a trace of background-accreted water in the blank experiment.

estimated properly if the UV absorption cross-section of H_2S ice is not well known. The infrared band strength of solid H_2S_2 was to our knowledge not reported in the literature, but it is expected to be lower than that of H_2S. Analyzing the infrared spectra of short UV irradiation of H_2S experiments (less than 1 minute irradiation to reduce the formation of secondary products like $HS_2^{\cdot}$ and S_2), we obtained a value of $A(H_2S_2)$ similar to that of $A(H_2S)$, but this estimation could be affected by a large error, mainly due to the small amount of product formed. We therefore used the value $A(H_2S_2) = 2.0 \times 10^{-17}$ cm molecule^{-1} to convert the integrated absorbance to the column density of produced H_2S_2, see fifth column of Table 1. The temperature-programmed desorption (TPD) data of X-ray irradiated H_2S ice, experiment N3, is shown in the top panel of Figure 2. The $m/z = 34$ peak corresponds to the tail of the desorption of H_2S that occurs around 95 K. Jiménez-Escobar & Muñoz Caro (2011) show an H_2S desorption temperature peaking at 84 K. This discrepancy is caused by the large difference in ice thickness; see, e.g., Acharyya et al. (2007) for a description of this phenomenon.

For comparison, the TPD data of the blank experiment with no irradiation, experiment N3, are shown in the bottom panel. The desorption peaks of $m/z = 64$ (S_2^+), 65 (HS_2^+), and 66 ($H_2S_2^+$) around 133 K are only observed in the X-ray-irradiated H_2S ice experiment. This value of the desorption

temperature agrees with that observed in UV irradiation of H_2S ice experiments (Grim & Greenberg 1987; Jiménez-Escobar & Muñoz Caro 2011), and the relative m/z values correspond to the fragmentation of H_2S_2 molecules impinging in the filament of the QMS after desorption from the irradiated ice during warm up. Formation of S_2 in our X-ray experiments, which would contribute to $m/z = 64$, is negligible because it would not account for $m/z = 65$ and 66 and desorbs at higher temperatures, above 200 K (Jiménez-Escobar & Muñoz Caro 2011). Therefore, the infrared and QMS data support the formation of H_2S_2 by soft X-ray irradiation of H_2S ice.

4. DISCUSSION AND ASTROPHYSICAL IMPLICATIONS

Soft X-ray processing of H_2S ice led to the formation of H_2S_2, as in UV irradiation and proton bombardment experiments (Jiménez-Escobar & Muñoz Caro 2011; Moore et al. 2007). In addition to H_2S_2, other species including S_2 were formed by UV irradiation of pure H_2S or H_2S in an H_2O ice matrix (Jiménez-Escobar & Muñoz Caro 2011). We show that for the same low-energy dose in absorbed eV molecule^{-1}, both X-ray and UV irradiation led to H_2S_2. The low X-ray flux used in our experiments resembles astrophysical conditions but the dose was insufficient to induce significant formation of $HS_2^{\cdot}$ and S_2 by photodissociation of the H_2S_2 product. Also, a higher X-ray flux would be required to easily detect photoproducts in experiments where H_2S is diluted in an H_2O ice matrix.

X-ray and UV irradiation of H_2S leading to H_2S_2, which photodissociates in the ice forming S_2, could explain the detection of S_2 in comets. Other S_2 formation channels appear to be less favorable. Formation of S_2 in the gas phase is unlikely as well as direct formation of S_2 from reaction of two S atoms in the ice. CS_2, the precursor of CS, has been proposed to lead also to S_2 (A'Hearn et al. 1983). However, the formation of S_2 should preferentially proceed by irradiation of H_2S, the molecule expected to be more abundant in ice mantles (Grim & Greenberg 1987) and up to 6–30 times more abundant than CS in comets (Biver et al. 2002; Bockelée-Morvan et al. 2010). The proposition of H_2S_2 as a parent molecule of S_2 in comets has implications for its formation in the nucleus or the coma. While gas phase photodissociation of H_2S_2 forms mainly SH radicals, in the solid phase the main product is S_2, formed by direct photodissociation or via the formation of HS_2 as an intermediate species (Isoniemi et al. 1999; Jiménez-Escobar & Muñoz Caro 2011). S_2 is therefore expected to be present in the nucleus, rather than formed in the coma. In addition, we observed experimentally that CS_2, H_2S_2, and S_2 have similar desorption temperatures and would be released to the coma almost simultaneously explaining the observed coma composition.

The production of S_2 in comet IRAS-Araki-Alcock 1983d was 2×10^{25} molecules s^{-1}, about 5×10^{-4} that of OH (A'Hearn et al. 1983). For comet Hyakutake, the production rate was between 6.5×10^{24} and 1.0×10^{25} molecules s^{-1} and an abundance of $(5–9) \times 10^{-3}$ relative to water (Laffont et al. 1998). To estimate the X-ray fluence required to form the S_2 observed in comets, we can compare the S_2/H_2S abundance ratio to experiments. For Hyakutake, the production rate of H_2S was $(0.45 \pm 0.2) \times 10^{27}$ molecules s^{-1} measured on April 10–12, and therefore $S_2/H_2S \sim 0.018$. For comet IRAS-Araki-Alcock, the S_2/CS abundance ratio was 1.0, but the abundance of H_2S was not measured, and we assume an average cometary value of $H_2S/CS = 6.25$ (Biver et al. 2002). Therefore,

$$\frac{S_2}{H_2S} = \frac{S_2}{CS} \times \left[\frac{H_2S}{CS}\right]^{-1} = 0.16. \quad (6)$$

The same value varies from 0.033 to 0.41, if we consider $S_2/H_2O = 5 \times 10^{-4}$ (A'Hearn et al. 1983) and $H_2S/H_2O =$ 0.12%–1.5% measured for 11 comets (Biver et al. 2002). The value $S_2/H_2S \sim 0.018$ of comet Hyakutake is more reliable because it was obtained from direct observations of this comet. This value is about 5.5 times larger than that obtained in X-ray experiment N3 of Table 1 for H_2S_2/H_2S. Therefore, a dose of at least $0.05 \times 5.5 = 0.28$ eV molecule^{-1} would be required to account for the observed S_2 abundance if all the H_2S_2 molecules are converted to S_2. For UV photons, assuming an optically thin ice in the UV, this dose is 0.072 eV molecule^{-1}. If H_2S is diluted in an H_2O–ice matrix the required irradiation doses are expected to be higher, although at least for UV irradiation the S_2/H_2S ratio is not critically dependent on the initial H_2S concentration (Grim & Greenberg 1987). Assuming that the X-rays emitted by a young solar-type star at 10 AU account for $2 \times 10^{11-13}$ eV cm^{-2} s^{-1} (Ciaravella et al. 2011), a gas-to-ice ratio of 10^{-4} (e.g., Öberg et al. 2009), an estimated ice X-ray absorption of about 1% for a silicate-core grain of 0.1 μm size with a 0.01 μm thickness ice mantle, and an ice column density of the order of 10^{19} molecules cm^{-2} around low-mass protostars (Öberg et al. 2009), the X-ray dose of 0.28 eV required to account for the S_2 abundance observed in comets, see above, roughly corresponds to between $4.4 \times (10^5–10^3)$ yr for the lower and upper X-ray flux limits, respectively.

The results obtained in this work open a new route to the formation of S_2 in comets. UV photons likely irradiated submicron-sized pre-cometary grains in the local dense cloud or later in the solar nebula. More energetic photons or cosmic rays are required to process grain agglomerates leading to cometesimals. The presence of X-rays inside the cloud where the UV flux is low, about 10^4 photons cm^{-2} s^{-1} (Cecchi-Pestellini & Aiello 1992), the high X-ray flux produced by the young Sun, and the larger penetration depth of X-rays in the ice compared to UV photons, suggest that X-rays played a significant role in the formation of S_2 in comets, and that this molecule could be present in interstellar and circumstellar ice mantles, contributing to the observed sulfur depletion in these regions.

A.C. is grateful to the Director of OAPA, Dr S. Sciortino, for the financial support to our research activity. This work was also financed by projects AYA2008-06374, AYA2011-29375, and CONSOLIDER grant CSD2009-00038 funded by Spanish MICINN. We thank S. Varisco for technical support.

REFERENCES

Acharyya, K., Fuchs, G. W., Fraser, H. J., van Dishoeck, E. F., & Linnartz, H. 2007, A&A, 466, 1005
A'Hearn, M. F., Schleicher, D. G., & Feldman, P. D. 1983, ApJ, 274, L99
Biver, N., Bockelée-Morvan, D., Crovisier, J., et al. 2002, Earth Moon Planets, 90, 323
Bockelée-Morvan, D., Crovisier, J., Mumma, M. J., & Weaver, H. A. 2004, in Comets II, ed. M. C. Festou, H. U. Keller, & H. A. Weaver (Tucson, AZ: Univ. Arizona Press), 391
Bockelée-Morvan, D., Hartogh, P., Crovisier, J., et al. 2010, A&A, 518, L149
Bockelée-Morvan, D., Lis, D. C., Wink, J. E., et al. 2000, A&A, 353, 1101
Boissier, J., Bockelée-Morvan, D., Biver, D. N., et al. 2007, A&A, 475, 1131
Boogert, A. C. A., Schutte, W. A., Helmich, F. P., et al. 1997, A&A, 317, 929
Buckle, J. V., & Fuller, G. A. 2003, A&A, 399, 567
Cecchi-Pestellini, C., & Aiello, S. 1992, MNRAS, 258, 125

Ciaravella, A., Jiménez-Escobar, A., Muñoz-Caro, G. M., et al. 2011, ApJ, 746, L1
Ferrante, R. F., Moore, M. H., Spiliotis, M. M., & Hudson, R. L. 2008, ApJ, 684, 1210
Garozzo, M., Fulvio, D., Palumbo, M. E., & Strazzulla, G. 2010, A&A, 509, A67
Geballe, T. R., Baas, F., Greenberg, J. M., & Schutte, W. 1985, A&A, 146, L6
Grim, R. J. A., & Greenberg, J. M. 1987, A&A, 181, 168
Isoniemi, E., Khriachtchev, L., Pettersson, M., & Rasanen, M. 1999, Chem. Phys. Lett., 311, 47
Jiménez-Escobar, A., & Muñoz Caro, G. M. 2011, A&A, 536, A91
Laffont, C., Boice, D. C., Andernach, H., et al. 1996, BAAS, 28, 1094
Laffont, C., Boice, D. C., Moreels, G., et al. 1998, Geophys. Res. Lett., 25, 2749
Lee, L. C., Wang, X., & Suto, M. 1987, J. Chem. Phys., 86, 4353
Moore, M. H., Hudson, R. L., & Carlson, R. W. 2007, Icarus, 189, 409
Muñoz Caro, G. M., Jiménez-Escobar, A., Martín-Gago, J. Á., et al. 2010, A&A, 522, 108
Öberg, K. I., Bottinelli, S., & van Dishoeck, E. F. 2009, A&A, 494, L13
Palumbo, M. E., Tielens, A. G. G. M., & Tokunaga, A. T. 1995, ApJ, 449, 674
Ribas, I., Guinan, E. F., Güdel, M., & Audard, M. 2005, ApJ, 622, 680
Wakelam, V., Caselli, P., Ceccarelli, C., Herbst, E., & Castets, A. 2004, A&A, 422, 159
Wakelam, V., Caselli, P., Ceccarelli, C., et al. 2005, in Proc. The Dusty and Molecular Universe: A Prelude to Herschel and ALMA, ed. A. Wilson (ESA SP-577; Noordwijk, The Netherlands: ESA), 435